TTP97-30
hep-ph/9708231
August 1997

Effects of Jet Azimuthal Angular Distributions on Dijet Production Cross Sections in DIS

Erwin Mirkes and Stefan Willfahrt

Institut für Theoretische Teilchenphysik, Universität Karlsruhe, D-76128 Karlsruhe, Germany

Abstract

A Monte Carlo study of the azimuthal angular distribution around the virtual boson-proton beam axis for dijet events in DIS at HERA is presented. In the presence of typical acceptance cuts on the jets in the laboratory frame, the azimuthal distribution is dominated by kinematic effects rather than the typical $\cos\phi$ and $\cos 2\phi$ dependence predicted by the QCD matrix elements. This implies that the ϕ dependent part of the QCD matrix elements contributes even to the dijet production cross section. Neglecting this ϕ dependence leads to an error of about 5-8% in the production cross section for typical acceptance cuts in the laboratory frame. We also present first NLO results on the ϕ-decorrelation of the jets through NLO effects.

Jet production in deep inelastic scattering (DIS) is an important laboratory for testing our understanding of perturbative QCD. Good event statistics allow for precise measurements and thus for a variety of tests of our understanding of QCD dynamics. For quantitative studies one clearly needs to compare data with calculations which include next-to-leading order (NLO) QCD corrections. The importance of keeping the full helicity structure in such a calculation is demonstrated in this letter for the example of dijet production in DIS.

Dijet production in neutral current (NC) DIS lepton proton scattering proceeds via the exchange of an intermediate vector boson γ^*/Z. We denote the γ^*/Z momentum by q, its absolute square by Q^2, and use the standard scaling variables $x = Q^2/(2P \cdot q)$ and $y = P \cdot q / P \cdot l$. In Born approximation, the subprocesses

$$e(l) + q(p_0) \to e(l') + q(p_1) + g(p_2) \tag{1}$$
$$e(l) + g(p_0) \to e(l') + q(p_1) + \bar{q}(p_2) \tag{2}$$

contribute to the NC two-jet cross section. NLO effects will be discussed later. *In the absence of jet cuts in the laboratory frame*, the full leading order (LO) QCD matrix elements predict a typical azimuthal angular distribution of the jets of the form [1,2]

$$\frac{d\sigma}{d\cos\phi} = A + B\cos\phi + C\cos 2\phi \tag{3}$$

where ϕ denotes the azimuthal angle of the jets around the virtual boson direction. This angular distribution is determined by the gauge boson polarization: the coefficients A, B, C in Eq. (3) are linearly related to the nine polarization density elements $h_{mm'}$ of the exchanged gauge boson:

$$h_{mm'} = \epsilon^*_\mu(m) H^{\mu\nu} \epsilon_\nu(m') \qquad (m, m' = +, 0, -) \tag{4}$$

where

$$\epsilon_\mu(\pm) = \frac{1}{\sqrt{2}}(0; \pm 1, -i, 0) \qquad \epsilon_\mu(0) = (0; 0, 0, 1) \tag{5}$$

are the polarization vectors of the exchanged boson in the hadronic (*i.e.* boson-proton) center of mass frame (HCM) and $H^{\mu\nu}$ denotes the hadronic tensor for the contributing QCD processes in Eqs. (1,2). The coefficient A in Eq. (3) can be expressed in terms of the diagonal density matrix elements h_{00}, h_{++}, h_{--}, the coefficient B in terms of transverse-longitudinal interference matrix elements $h_{+0}, h_{0+}, h_{-0}, h_{0-}$ and the coefficient C in terms of transverse interference density matrix elements h_{+-}, h_{-+} [3]. Technically, the coefficient A can be calculated from the hadronic tensor in the one photon exchange case by the two covariant projections $g_{\mu\nu}$ and $p_{0\,\mu} p_{0\,\nu}$ on the hadronic tensor, whereas projections defined with final state hadronic momenta are necessary to calculate B and C [2].

The NLO $eP \to n$ jets event generator MEPJET [4] is used for the subsequent numerical studies in this paper. The corresponding cross sections and distributions are calculated by evaluating the corresponding one-loop and tree-level helicity amplitudes and therefore, the MEPJET program allows for the calculation of all possible jet-jet and jet-lepton correlations in NLO, including the ϕ dependence in Eq. (3).

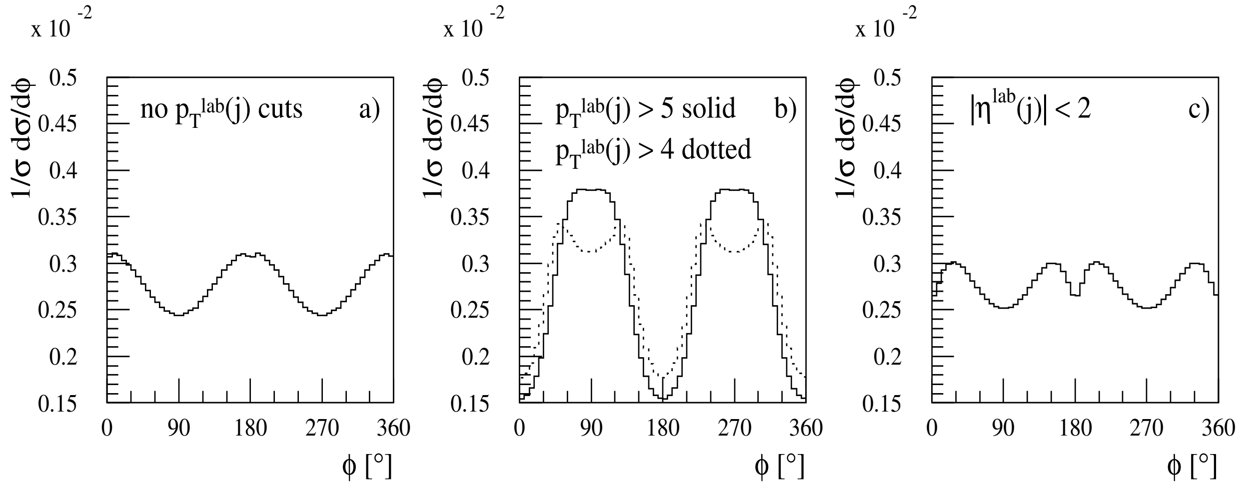

FIG. 1. a) Normalized ϕ distribution in LO around the virtual boson direction of jets in the cone scheme defined in the HCM with $p_T^{\rm HCM}(j) > 5$ GeV. The ϕ integrated dijet cross section is 1465pb; b) same as a) but but with an additional cut of $p_T^{\rm lab}(j) > 5$ (solid) ($p_T^{\rm lab}(j) > 4$ (dotted)) GeV on the jets. The ϕ integrated dijet cross section is 945 pb (1146 pb); c) same as a) but with an additional $|\eta^{\rm lab}(j)| < 2$ cut on the jets. The ϕ integrated dijet cross section is 1087 pb. All results are given in LO with γ^* and Z exchange.

The following numerical studies for e^+P scattering with γ/Z exchange are based on MRSR1 [5] parton distribution functions with the two loop formula for the strong coupling constant and $n_f = 5$. The renormalization and the factorization scales are set to $\mu_R = \mu_F = \langle k_T^B(j)\rangle$, the average k_T^B of the jets, which appears to be the "natural" scale for jet production in DIS [6]. Here, $(k_T^B(j))^2$ is defined by $2\,E_j^2(1-\cos\theta_{jP})$ in the Breit frame, where the subscripts j and P denote the jet and proton, respectively. The lepton and hadron beam energies are 27.5 and 820 GeV, respectively and events are selected in the following kinematical region: 40 GeV$^2 < Q^2 <$ 2500 GeV^2, $0.04 < y < 1$, and $E(e') > 10$ GeV, where $E(e')$ is the energy of the scattered lepton. Unless stated otherwise, no cuts on the pseudo-rapidity $\eta^{\rm lab} = -\ln\tan(\theta/2)$ or the transverse momentum on the jets in the lab frame are imposed.

Without an (experimental) separation of a quark, anti-quark or gluon jet, the $\cos\phi$ term in Eq. (3) is not observable and thus has to be averaged out. The resulting LO $\cos 2\phi$ dependence of dijet events is shown in Fig. 1a for a cone scheme defined in the HCM with radius $R=1$ and $p_T^{\rm HCM}(j) > 5$ GeV. We find very similar results for jets in the k_T algorithm [8] implemented in the Breit frame with $E_T^2 = 40$ GeV^2 and $y_{\rm cut} = 1$. Note that the HCM and the Breit frame are related by a boost along the boson-proton direction which does not change the ϕ dependence in Eq. (3). One observes a sizable $\cos 2\phi$ dependence (after averaging over $\cos\phi$) in Fig. 1a as expected from Eq. (3). The size of the ϕ dependence in this normalized distribution is rather insensitive on the $p_{T\,\rm min}^{\rm HCM}$ (or E_T in the k_T scheme) requirements on the jets. Averaging (integrating) over ϕ implies that the coefficients B and C in Eq. (3) do not contribute to the dijet production cross section in this case.

Fig. 1b shows the ϕ distribution of the jets defined in the cone scheme and cuts as in Fig. 1a, but with an additional $p_T^{\rm lab}(j) > 5$ (solid) ($p_T^{\rm lab}(j) > 4$ (dotted)) GeV cut on the jets in the laboratory frame. Only 65% (78%) of the events pass the additional $p_T^{\rm lab}(j)$

TABLE I. Effects of the jet azimuthal angular distribution on the dijet production cross section in DIS as a function of $p_T^{\rm lab}(j)$ cuts on the jets. $\sigma^{\rm exact}$ ($\sigma^{\rm approx}$) is based on the exact (approximate) matrix elements including (without) the coefficients B and C in Eq. (3). Jets are defined in the HCM with radius $R=1$ and and $p_T^{\rm HCM}(j) > 5$ GeV. Additional parameters are explained in the text. Similar results are found for jets defined in the k_T scheme.

lab frame cut	$\sigma^{\rm exact}$[2-jet]	$\sigma^{\rm approx}$[2-jet]	$\Delta\sigma = [\sigma^{\rm approx} - \sigma^{\rm exact}]/\sigma^{\rm exact}$
$p_T^{\rm lab}(j) > 0$	1465 pb	1465 pb	0 %
$p_T^{\rm lab}(j) > 2$	1390 pb	1405 pb	1.1 %
$p_T^{\rm lab}(j) > 4$	1145 pb	1195 pb	4.4 %
$p_T^{\rm lab}(j) > 6$	689 pb	733 pb	6.4 %
$p_T^{\rm lab}(j) > 8$	348 pb	370 pb	6.3 %
$p_T^{\rm lab}(j) > 10$	187 pb	198 pb	5.9%

TABLE II. Same as table I as a function of $|\eta^{\rm lab}(j)|$ cuts on the jets.

lab frame cut	$\sigma^{\rm exact}$[2-jet]	$\sigma^{\rm approx}$[2-jet]	$\Delta\sigma = [\sigma^{\rm approx} - \sigma^{\rm exact}]/\sigma^{\rm exact}$
$\|\eta^{\rm lab}(j)\| < 5$	1465 pb	1465 pb	0 %
$\|\eta^{\rm lab}(j)\| < 3.5$	1437 pb	1439 pb	0.15%
$\|\eta^{\rm lab}(j)\| < 2.5$	1282 pb	1288 pb	0.5%
$\|\eta^{\rm lab}(j)\| < 1.5$	801 pb	820 pb	2.4%
$\|\eta^{\rm lab}(j)\| < 0.5$	131 pb	141 pb	7.6%

cuts. These cuts have a dramatic effect on the shape of the ϕ distribution. The shape of the distribution is now governed by the kinematics of the surviving events. The $p_T^{\rm lab}(j)$ cut introduces a strong ϕ dependence. The "kinematical" ϕ distribution in Fig. 1b is very different from the "dynamical" $\cos 2\phi$ distribution in Fig. 1a. The only remaining vestiges of the gauge boson polarization effects in the ϕ distribution are the dips at $\phi = 90^\circ$ and 270° in the dotted curve in Fig. 1b. Imposing cuts on the pseudo-rapidities $|\eta^{\rm lab}(j)|$ of the jets in the laboratory frame has also a large effect on the shape of the ϕ distribution as shown in Fig. 1c.

A consequence of this kinematical ϕ dependence is, that the ϕ dependent coefficients B and C in Eq. (3) now also contribute to the dijet *production* cross section after integration over ϕ. We have analyzed this effect by comparing the dijet cross section using the exact matrix elements (including the ϕ dependent coefficients in Eq. (3)) with the resulting dijet cross section where the coefficients B and C in the matrix elements in Eq. (3) are neglected. The results are shown in table I for various $p_T^{\rm lab}(j)$ cuts on the jets. We find that the dijet cross section based on the approximate matrix elements is larger compared to the correct result. The error depends on the $p_T^{\rm lab}(j)$ cuts and can reach about 6.5 %. The error from the approximate matrix elements in the presence of pseudo-rapidity cuts on the jets in the lab frame is shown in Table II. A combination of $p_T^{\rm lab}(j)$ and $|\eta^{\rm lab}(j)|$ cuts can lead to even larger effects.

Let us now discuss some NLO effects on the dijet azimuthal angular distribution in e^+P

scattering with γ/Z exchange, where the full helicity structure is kept. The NLO $\mathcal{O}(\alpha_s^2)$ 2-jet cross section receives contributions from the one-loop corrections to the Born processes in Eqs. (1) and (2) and from the integration over the unresolved region (defined by a given jet algorithm) of the 3-parton final state tree level matrix elements

$$e(l) + q(p_0) \to e(l') + q(p_1) + g(p_2) + g(p_3) \tag{6}$$

$$e(l) + q(p_0) \to e(l') + q(p_1) + q(p_2) + \bar{q}(p_3) \tag{7}$$

$$e(l) + g(p_0) \to e(l') + q(p_1) + \bar{q}(p_2) + g(p_3) \tag{8}$$

and the corresponding antiquark processes with $q \leftrightarrow \bar{q}$.

The NLO corrections introduce a new (numerically small) additional $\sin\phi$ and $\sin 2\phi$ dependence in the NC cross section in Eq. (3) through the imaginary parts of the one-loop contributions [7].

In addition, the tree level contributions to dijet production in Eqs. (6-8) imply that the two jets are no longer necessarily back-to-back in ϕ like in LO, *i.e.* one expects $\Delta\phi = |\phi(\text{jet } 1) - \phi(\text{jet } 2)| \neq 180^\circ$. A deviation from $\Delta\phi = 180^\circ$ can arise for example in the cone scheme if one of the three final state partons is well separated in ΔR from the other two partons but does not pass the acceptance cuts (like the $p_T^{\text{HCM}}(j) > 5$ GeV cut), whereas the remaining two partons passes all jet requirements. Thus the event will be accepted as a two-jet event where the jets are, however, no longer balanced in ϕ.

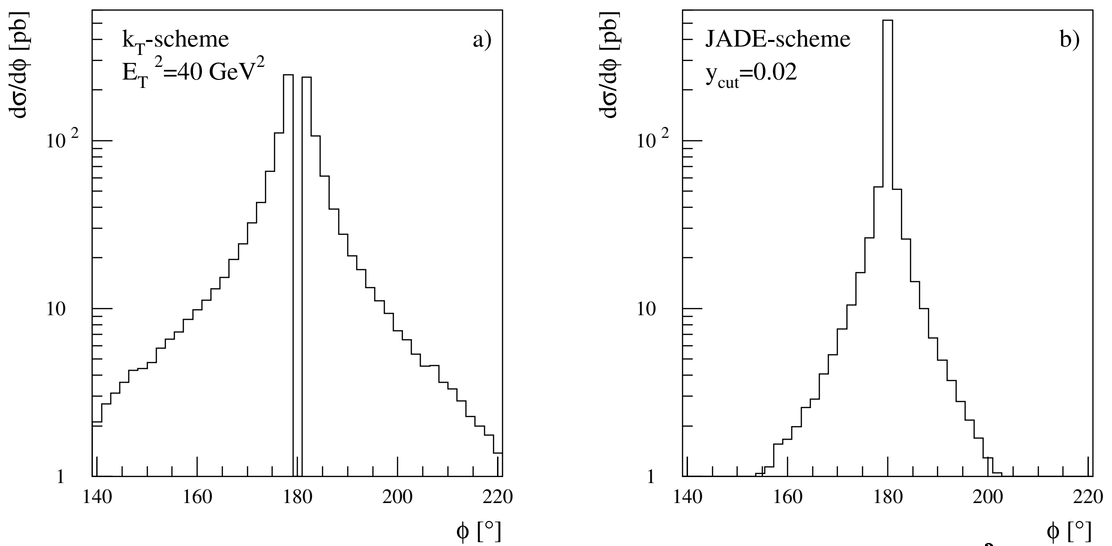

FIG. 2. a) $\Delta\phi$ distribution in NLO for jets defined in the k_T scheme with $E_T^2 = 40$ GeV^2. Similar results are found for jets in the cone scheme defined in the HCM. b) same as a) for the JADE scheme and $y_{\text{cut}} = 0.02$.

The effect is shown in Fig. 2 for the k_T scheme defined in the Breit frame with $E_T^2 = 40$ GeV^2 (Fig. 2a) and the JADE scheme [9,2] defined in the lab frame with $y_{\text{cut}} = 0.02$ (Fig. 2b). In the latter case, jets are required to have a minimum transverse momentum of 2 GeV in the HCM and the lab frame. The corresponding NLO (LO) cross sections are 1350 pb (1240 pb) in the k_T scheme and 1570 pb (970 pb) in the JADE scheme.

Fig. 2 illustrates that the decorrelation effect through the NLO corrections depends strongly on the chosen jet algorithm. The decorrelation is larger in the k_T scheme (or a cone scheme) than in the JADE scheme. Note that the central bin around 180° in Fig. 2a has a negative weight. This shows that the fixed NLO predictions are not infrared save for $\Delta\phi$ close to 180°. This effect is caused by the negative contributions from the virtual corrections, which contribute only to this bin due to the Born kinematics. For the JADE scheme the negative contributions in the central bin are already overcompensated by the positive tree-level contributions in Eqs. (6-8). Since the decorrelation effect is larger in Fig. 2a, one has either to choose wider bins in $\Delta\phi$ for the k_T scheme to arrive at a positive result in the central bin or alternatively one would have to use resummation techniques to obtain a reliable perturbation expansion close to $\Delta\phi$=180°.

Finally, the small asymmetry in the $\Delta\phi$ decorrelation in Fig. 2 is caused by our fixed ordering of jet 1 and jet 2. The distributions would be perfectly symmetric without a separation of a quark, anti-quark or gluon jet.

To summarize: The azimuthal angular distribution of dijet events around the boson proton direction has been discussed. In the presence of cuts on the jets in the lab frame, the angular distribution is dominated by kinematic effects and the residual dynamical effects from the gauge boson polarization are small. The kinematic effects imply that the non-diagonal helicity density matrix elements of the exchanged boson, which are fully taken into account in the NLO event generator MEPJET, contribute also to the dijet production cross section. First studies of the dijet angular decorrelation through NLO corrections show a fairly strong dependence on the chosen jet algorithm.

REFERENCES

[1] H. Georgi, H. D.Politzer, Phys. Rev. Lett. **40** (1978) 3;
G. Köpp, R. Maciejko, P. M. Zerwas, Nucl. Phys. **B144** (1978) 123;
A. Mendez, A. Raychaudhuri, V.J. Stenger, Nucl. Phys. **B148** (1979) 499;
V. Hedberg, G. Ingelmann, C. Jacobson, L. Jönsson, "Proceedings of the 1991 HERA Physics Workshop".

[2] J.G. Körner, E. Mirkes and G. Schuler, Int. J. Mod. Phys. **A4** (1989) 1781.

[3] T. Brodkorb and E. Mirkes, Z. Phys. **C66** (1995) 141, [hep-ph/9404287].

[4] E. Mirkes and D. Zeppenfeld, Phys. Lett. **B380** (1996) 105, [hep-ph/9511448].

[5] A.D. Martin, R.G. Roberts and W.J. Stirling, Phys. Lett. **B387** (1996) 419, [hep-ph/9606345].

[6] E. Mirkes and D. Zeppenfeld, *Nucl. Phys.* **B** (Proc. Suppl.) **51C** (1996) 273; [hep-ph/9606332]; see also in "Proceedings of the 1996 HERA Physics Workshop" [hep-ph/9609274].

[7] K. Hagiwara, K. Hikasa and N. Kai, Phys. Rev. **D27** (1983) 84.

[8] S. Catani, Y.L. Dokshitzer and B.R. Webber, Phys. Lett. **B285** (1992) 291.

[9] JADE Collaboration, W. Bartel et al. Z. Phys. **C33** (1986) 23.